the thin shell structure can be simplified. A procedure is proposed to analyze shell structure behavior.

2. CONCEPT OF VFIFE

VFIFE is based on structural mechanics and avoids the difficulty of solving the iterative equations of partial differential equations in traditional nonlinear structure analysis. The concepts in VFIFE are: (1) point description, (2) path element and (3) convected material frame.

During the analyzed time interval of the motion of particles, the Euler's law of motion is applied, and the internal membrane forces and moments are calculated using constant strain triangular (CST) element and discrete Kirchhoff triangular (also called VFIFE-DKT in this paper) element (Batoz et al. 1980) under the deformation coordinate respectively.

2.1 Point Description, Path Element and Convected Material Frame

The analyzed structure is discretized as finite particles. The space surrounding with particles is an element. The governing equations in motion analysis are a set of equations that describe the movement of particles over time. Path element is a small time interval which is used to describe the process of particle motion. The structure elements will perform small deformation and small rotation in each path element. Then, in each path element, the mechanics of the materials and engineering mechanics can be applied. The trajectory of the particles over the analyzed time are used to describe the structure deformation in the analyzed space, as shown in Figure 1.

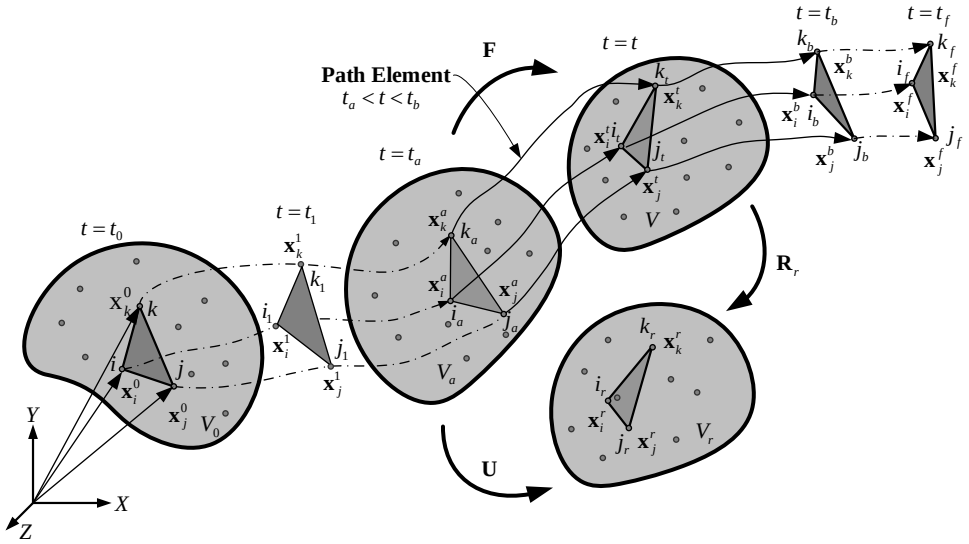

Fig. 1 Point description, path element and convected material frame

During each path element, there are four configurations to analyze. The structure at the initial state $t = t_0$ is V_0 , at $t = t_a$ is the reference configuration V_a , the current configuration at time t is V_t, and the virtual configuration is V_r .

The relative position vector $d\mathbf{x}$ in the current configuration can be represented by the relative position $d\mathbf{x}_a$ of the deformation gradient and the reference configuration,

$$d\mathbf{x} = \mathbf{F}d\mathbf{x}_a = \mathbf{R}\mathbf{U}d\mathbf{x}_a \tag{1}$$

The relative position vector $d\mathbf{x}_r$ under the virtual configuration V_r can be represented by the relative position of the predicted deformation gradient and the current configuration, or by the relative position of the reverse rigid body rotation matrix and the current configuration,

$$d\mathbf{x}_r = \mathbf{F}_r d\mathbf{x} = \mathbf{R}_r^T d\mathbf{x} \tag{2}$$

Substitute equation (1) into equation (2), and the inverse rigid body rotation matrix in the virtual configuration is approximated by the rigid body rotation matrix,

$$d\mathbf{x}_r = \mathbf{F}_r\mathbf{F}d\mathbf{x}_a = \left(\mathbf{R}_r^T\mathbf{R}\right)\mathbf{U}d\mathbf{x}_a \cong \mathbf{U}d\mathbf{x}_a \tag{3}$$

For a deformable body, the initial configuration V_a in the path element is used to be the reference configuration of deformation of the structure. The reference configuration is updated in each path element, so the estimated motion will be updated. This is the convected material frame which is the basic concept of motion analysis.

2.2 Governing Equations

As shown in Fig. 2, each particle is subjected to internal forces and external forces. Based on the Euler's law of motion, the motion of each particle is represented by the independent equations,

$$\overline{\mathbf{m}}_i\ddot{\mathbf{u}}_i = \mathbf{F}_i - \mathbf{f}_i \tag{4}$$

$$\bar{\mathbf{I}}_i\ddot{\boldsymbol{\beta}}_i = \mathbf{M}_i - \mathbf{m}_i \tag{5}$$

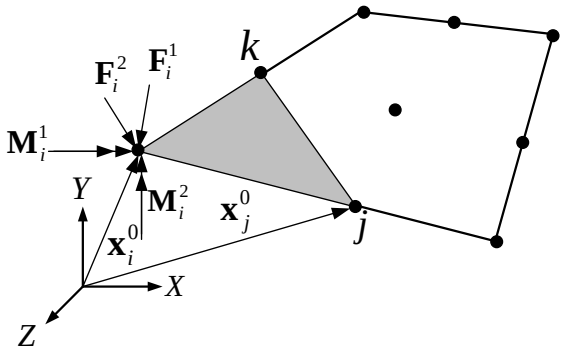

(a) A shell structure subjected to external forces

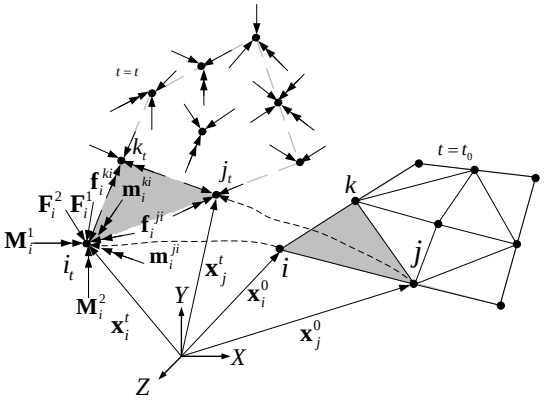

(b) Particles subjected to external forces and internal forces

Fig. 2 Internal forces on particles and structure

The mass matrix in equation (4) use the concept of lump mass, and the mass moment of inertia in equation (5) is calculated from the plate mass moment of inertia.

3. Motion analysis of VFIFE-DKT

Element deformation only relate to the pure deformation in the deformation coordinate. The rigid body motion must be removed from the displacement and rotation of the shell element. Reverse rigid body motion, deformation coordinate and convected material frame is performed in the calculation of the element internal forces.

3.1 Reverse Rigid Body Motion

As shown in Fig. 3, at time t , the unit normal $\mathbf{n}$ is calculated from the triangular shell element formed by the particles i' , j' , and k' . The virtual configuration V_r (element can be determined by the reverse rigid body translation and rotation of the current configuration V_t . In addition, the rigid body rotation is calculated using the quaternion rotation (Hamilton 1853, Dam et al. 1998, Kuipers 1999). The centroid of the element C_a is selected as a reference point. Therefore, the total rigid body rotation vector of the element is

$$\boldsymbol{\theta} = q_2 q_1 \tag{6}$$

where q_1 and q_2 are the out-of-plane rotation and in-plane rotation respectively. The quaternion is composed of in-plane rotation and in-plane rotation.

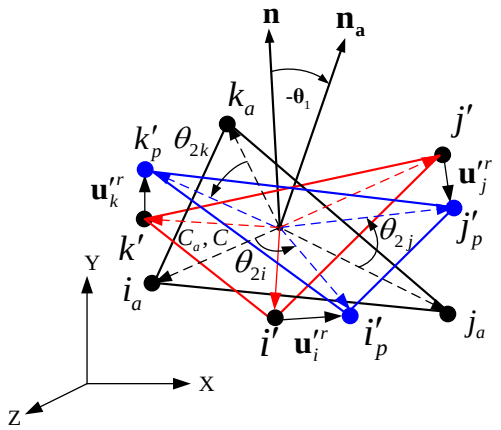

Fig. 3 Reverse rigid body motion of an element

3.2 Deformation Coordinate

After the removal of the rigid body motion, the current configuration has been moved to the reference configuration. In order to calculate the deformation, deformation coordinate $(\hat{x}, \hat{y}, \hat{z})$ has been set up and the coordinate origin is set at one of the particles of the reference configuration. In Figure 4, the three base vectors $(\hat{\mathbf{e}}_1, \hat{\mathbf{e}}_2, \hat{\mathbf{e}}_3)$ of the deformation coordinate can be defined as

$$\hat{\mathbf{e}}_1 = \frac{\boldsymbol{\eta}_j^d}{\left|\boldsymbol{\eta}_j^d\right|} \tag{12}$$

$$\hat{\mathbf{e}}_3 = \mathbf{n}_a \tag{13}$$

$$\hat{\mathbf{e}}_2 = \frac{\hat{\mathbf{e}}_3 \times \hat{\mathbf{e}}_1}{\left|\hat{\mathbf{e}}_3 \times \hat{\mathbf{e}}_1\right|} \tag{14}$$

The transformation matrix $\mathbf{Q}$ is defined as

$$\mathbf{Q} = \left\{\hat{\mathbf{e}}_1 \quad \hat{\mathbf{e}}_2 \quad \hat{\mathbf{e}}_3\right\}^T \tag{15}$$

The transformation matrix $\mathbf{Q}$ is used to transform parameters (such as position vectors, displacements and forces) from global coordinate system to deformation coordinate system.

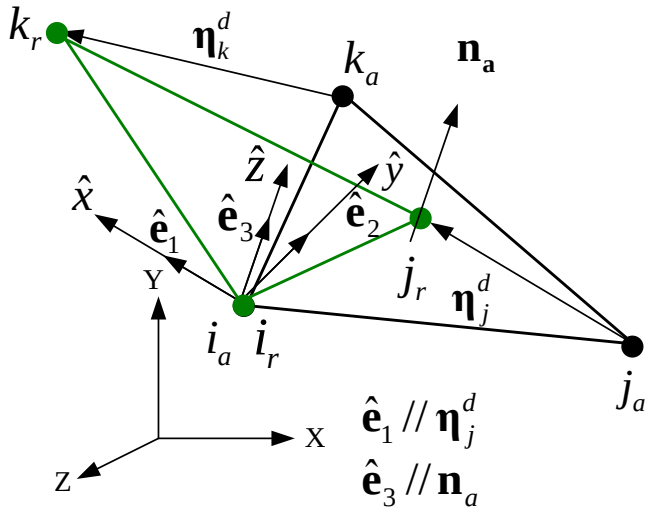

Fig. 4 Element deformation and deformation coordinate

3.3 Virtual Work and Virtual Strain Energy

In VFIFE, the equivalent internal forces of the shell element from pure deformation between reference configuration and current configuration is calculated in the deformation coordinate system ($\hat{x}, \hat{y}, \hat{z}$). Since the internal virtual work δW induced from internal force which is equal to the virtual strain energy δU from deformation, the internal force can be calculated. In addition, the virtual strain energy is also composed of membrane effect and bending effect,

$$\delta U = \delta U_m + \delta U_b \tag{16}$$

and,

$$\delta U_m = \int_{\hat{V}} \delta \hat{\varepsilon}_m^T \hat{\sigma}_m d\hat{V} \tag{17}$$

$$\delta U_b = \int_{\hat{V}} \delta \hat{\varepsilon}_b^T \hat{\sigma}_b d\hat{V} \tag{18}$$

where $\hat{\varepsilon}_m$ and $\hat{\varepsilon}_b$ are the membrane and bending strains respectively, and correspond to the normal and bending stresses.

3.4 Internal Membrane Force

The equivalent internal forces associated with the deformation of membrane and bending effects of the element in the deformation coordinate is calculated from the equivalent of virtual work and virtual strain energy. The internal membrane forces and bending moments are calculated from the followings

$$\hat{\mathbf{f}}^* = \int_{V_\varepsilon} \mathbf{B}_m^T \hat{\boldsymbol{\sigma}}_m dV = \left\{ \hat{f}_{jx} \quad \hat{f}_{kx} \quad \hat{f}_{ky} \right\} \tag{19}$$

$$\hat{\mathbf{m}} = \left(2A_a \int_0^1 \int_0^{1-\hat{\lambda}} \mathbf{B}_m^T \mathbf{D}_b \mathbf{B}_m dA_a \right) \mathbf{d}_b^T = \left\{ \hat{m}_{ix} \quad \hat{m}_{iy} \quad \hat{m}_{jx} \quad \hat{m}_{jy} \quad \hat{m}_{kx} \quad \hat{m}_{ky} \right\} \tag{20}$$

Internal moments can be directly determinate from equation (20). The remaining three internal membrane forces can be further determined from the equilibrium equations. The shear forces induced from bending effect can be also determined from the equilibrium equation of moments and shear forces.

3.5 Internal Moment and Internal Force

As shown in Fig. 5 and Fig. 6, in deformation coordinate, six in-plane forces from CST element, three shear forces and six moments of the bending effect from the VFIFE-DKT element are obtained from the derivation in the previous section. To perform all analyses in the current configuration V_t in global coordinate system, all forces and moments represented in the virtual configuration V_r in the deformation coordinate system must be transformed into global coordinates. The internal forces and moments in the deformation coordinate are

$$\hat{\mathbf{f}}_n = \left\{ \hat{f}_{ix} \quad \hat{f}_{iy} \quad \hat{f}_{iz} \quad \hat{f}_{jx} \quad \hat{f}_{jy} \quad \hat{f}_{jz} \quad \hat{f}_{kx} \quad \hat{f}_{ky} \quad \hat{f}_{kz} \right\}^T \tag{21}$$

$$\hat{\mathbf{m}}_n = \left\{ \hat{m}_{ix} \quad \hat{m}_{iy} \quad 0 \quad \hat{m}_{jx} \quad \hat{m}_{jy} \quad 0 \quad \hat{m}_{kx} \quad \hat{m}_{ky} \quad 0 \right\}^T \tag{22}$$

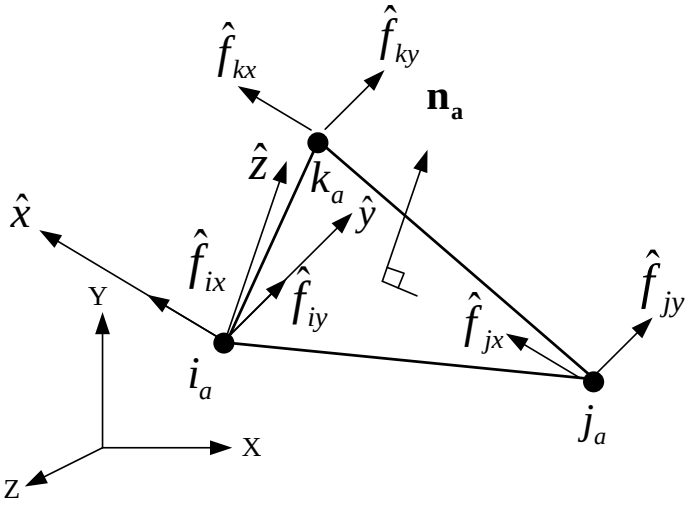

Fig. 5 Internal membrane forces on CST element

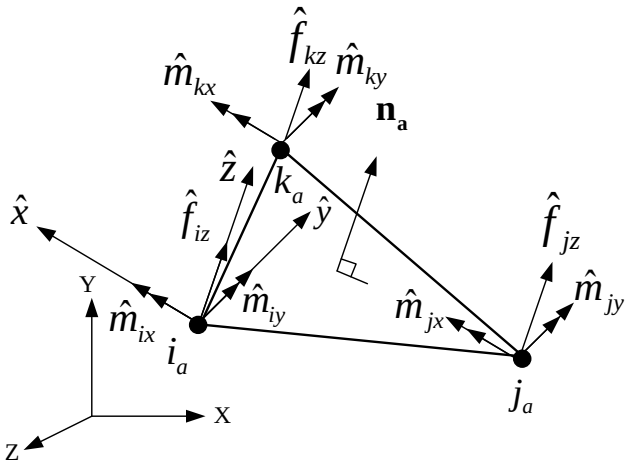

Fig. 6 Internal shear forces and moments on VFIFE-DKT element

These internal forces and moments in global coordinate will be introduced to equation (4) and (5). Apply central difference method, the displacements and rotations solved from equation (4) and (5) will be the initial value of the next path element.

4. NUMERICAL EXAMPLES

In this section, two numerical examples are performed to illustrate the accuracy of the VFIFE-DKT element. The first example is the twisted beam problem to verify the accuracy when the shell is warped. The second example is the hemispherical shell which has finite rotations and large rigid body motions analysis to verify the ability of VFIFE to handle this kind of problem.

4.1 Twisted Beam

This example is often used to verify the ability of the shell element to obtain correct response when the shell is warped. The analyzed structure with a 12×2(×2) mesh is described in Figure 7. The beam is applied a load (see Fig. 8) at one end and clamped at the other end. The end displacement of the beam is calculated. As shown in Fig. 9, VFIFE performs very well accuracy compare to the result of Wu et al. (2005).

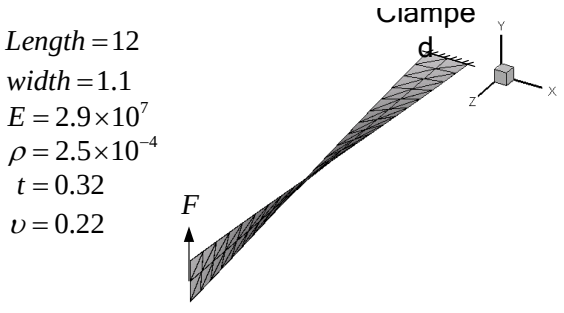

Fig. 7 Beam layout

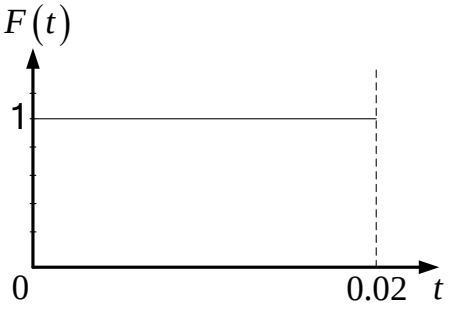

Fig. 8 External load history applied on the twisted beam

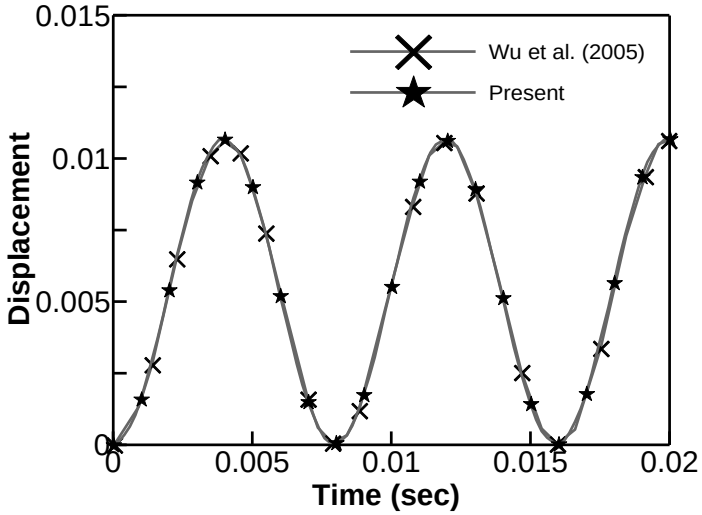

Fig. 9 End displacement of the beam

4.2 Hemispherical Shell

This example assesses the ability of element to handle finite rotations and large rigid body motions. As shown in Fig. 10, the geometrical dimensions of the hemispherical shell are radius $R=10$ and thickness $t=0.4$. The material properties are taken as Young's modulus $E=6.285\times10^{7}$, Poisson's radio $\nu=0.3$ and density $\rho=2.5\times10^{-4}$. The damping is not considered. Due to the symmetry of the geometry and loading, only consider a quarter of the hemispherical shell and 114 elements in modeling. Constant loads are applied at two points as shown in Fig. 11. The exact solution for the static radial displacement at the loading points is 0.0924 from Wu et al. (2005). The VFIFE calculation nresults are shown in Fig. 12. It can be shown that VFIFE provides good results in this calculation compare with Wu et al. (2005) and Zheng et al. (2011).

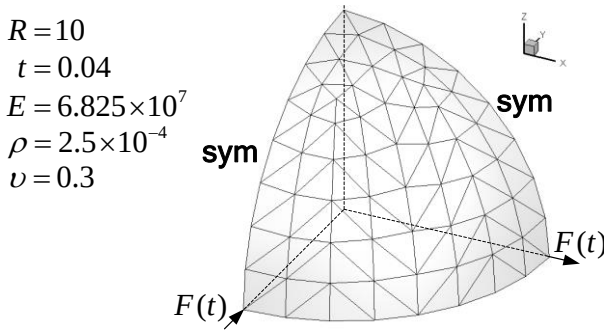

Fig. 10 Geometry and material properties of hemispherical shell

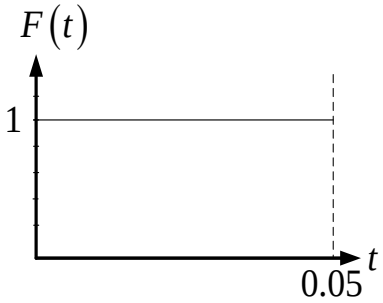

Fig. 11 Load history

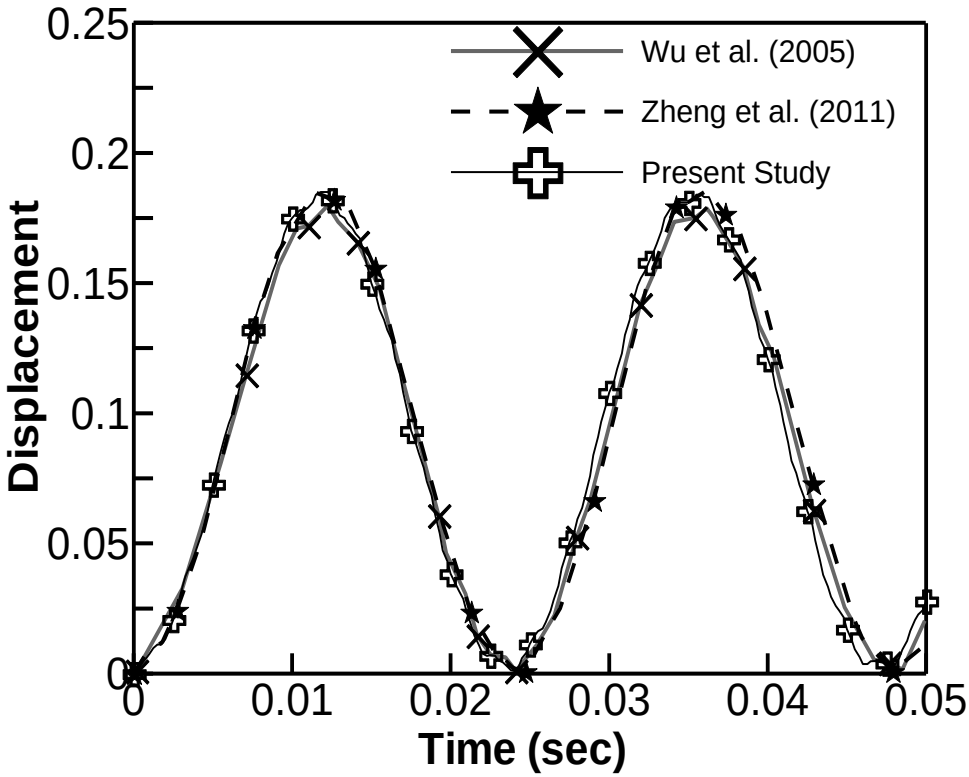

Fig. 12 Free end displacements of the thin plate

5. CONCLUSIONS

In this paper, a new method Vector Form Intrinsic Finite method (VFIFE) based on particle calculation internal force is developed, which is applied to the motion analysis of thin shell structures. VFIFE can be used to calculate large displacement and large rotation of nonlinear motion of thin shell structures. Using the point description, path element, reverse rigid body motion and convected material frame, the complex motion problem can be analyzed effectively. The finite rotation theory is adopted to effectively remove the displacement caused by the rigid body during rapid vibration. In numerical examples, the VFIFE verified that the results maintain convergence, accuracy in the analysis of thin shell structures with large deformations.

REFERENCES

Bathe K.J. and Bolourchi S. (1980), “A geometric and material nonlinear plate and shell element,” Comput. Struct., **11**(1), 23-48, 1980.
Batoz, J.L. (1982), "An explicit formulation for an efficient triangular plate-bending element," Int. J. Numer. Meth. Eng., **18**(7), 1077-1089.
Battini J.M. and Pacoste C. (2006), "On the choice of the linear element for corotational triangular shells," Comput. Method Appl. M., **195(**44), 6362-6377.
Li Z. and Vu-Quoc L. (2007), "An efficient co-rotational formulation for curved triangular shell element," Int. J. Numer. Meth. Eng., **72(**9), 1029-1062.
Norachan P., Suthasupradit S., and Kim K.D. (2012), "A co-rotational 8-node degenerated thin-walled element with assumed natural strain and enhanced assumed strain," Finite Elem. Anal. Des, **50**, 70-85.
Ting E.C., Shih C. and Wang Y.K. (2004), "Fundamentals of a vector form intrinsic finite element: Part I. Basic procedure and a plane frame element," J. Mech., **20(**2), 113-122.
Ting E.C., Shih C. and Wang Y.K. (2004), "Fundamentals of a vector form intrinsic finite element: Part II. plane solid elements," J. Mech., **20(**2), 123-132.
Batoz J.L., Bathe K.J. and Ho L.W. (1980), "A study of three-node triangular plate bending elements," Int. J. Numer. Meth. Eng., **15(**12), 1771-1812.
Hamilton W.R. (1853), Lectures on quaternions. Hodges and Smith.
Dam E.B., Koch M. and Lillholm M. (1998), Quaternions, interpolation and animation. Datalogisk Institut, Københavns Universitet Copenhagen.
Kuipers J.B. (1999), Quaternions and rotation sequences. Princeton university press Princeton.
Wu S., Li G.Y. and Belytschko T. (2005), “A DKT shell element for dynamic large deformation analysis,” Commun. Numer. Meth. Engng., **21,** 651–74.
Zheng G., Cui X., Li G. and Wu S. (2011), “An edge-based smoothed triangle element for non-linear explicit dynamic analysis of shells”. Comput. Mech., **48**(1), 65-80.